Theoretical Modelling of Hierarchically Associated Structures in Hydrophobically Modified PNIPAM Aqueous Solutions on the Basis of a Neutron Scattering Study

Tsuyoshi Koga,[*1] *Fumihiko Tanaka,*[1] *Ryuhei Motokawa,*[2] *Satoshi Koizumi,*[2] *Françoise M. Winnik*[3]

Summary: We developed a theoretical model for a self-assembling telechelic poly(*N*-isopropylacrylamide) (PNIPAM) carrying octadecyl end-groups in aqueous solution, as a function of temperature and concentration, on the basis of small-angle neutron scattering data. In solutions of concentration 10 g L^{-1} at temperatures between 10 and 20 °C, the telechelic PNIPAM of molecular weight of 22,200 g mol^{-1} associates in the form of flower micelles containing about 12 polymer chains. Micelles have a 3-layered core-shell morphology with an inner core consisting of the octadecyl units, a dense inner shell consisting of partly collapsed PNIPAM chains, and an outer shell of swollen hydrated PNIPAM chains. Drastic changes in the scattering profile of the solution heated above 31 °C are attributed to the formation of mesoglobules of diameter of 100 nm consisting of about 1000 polymer chains. In solutions of lower concentration (1 g L^{-1}), association of flower micelles and mesoglobules is suppressed. The structure of the individual flower micelles and mesoglobules is not affected by changes in concentration. In solutions of 50 g L^{-1}, a peak attributed to a correlation between flower micelles appears in the scattering profiles at low temperature (10 °C). Despite the difference in the population of intermicellar bridges, the overall temperature dependence of the scattering profile at 50 g L^{-1} remains similar to that at 10 g L^{-1}.

Keywords: flower micelle; hydrophobically modified poly(*N*-isopropylacrylamide); mesoglobule; modelling; neutron scattering

Introduction

Associating polymers form a variety of self-assembled structures in water, depending on the temperature and the polymer concentration. Typical examples of such structures are flower micelles and physical gels with micellar junctions.[1–3] Telechelic associating polymers, consisting of a hydrophilic main chain flanked by two hydrophobic end-groups, have been used as typical and simple models of well-defined associating polymers to study and understand the self-assembly[3–5] and rheological[6,7] properties of such systems. Most of these studies have been carried out under conditions for which the polymer chain is regarded as highly soluble in water, as in the case of hydrophobically modified poly(ethylene oxide)s.

Recently, F. Winnik and coworkers reported the preparation of associative polymers consisting of a poly(*N*-isopropylacrylamide) (PNIPAM) chain carrying

[1] Department of Polymer Chemistry, Graduate School of Engineering, Kyoto University, Kyoto 615-8510, Japan
Fax: (+81) 75 383 2707;
E-mail: tkoga@phys.polym.kyoto-u.ac.jp
[2] Soft Matter & Neutron Scattering Group, ASRC, JAEA, Ibaraki, 319-1195, Japan
[3] Department of Chemistry and Faculty of Pharmacy, University of Montréal, CP 6128, Montreal QC, H3C 3J7, Canada

alkyl groups at each chain end (tel-PNIPAM), and studied the self-assembled structures and phase behavior in aqueous solutions of these tel-PNIPAMs.[8–11] Since the PNIPAM homopolymer is a thermo-responsive polymer undergoing a coil-to-globule transition at 32 °C in water,[12] tel-PNIPAMs are expected to exhibit interesting structural and dynamic properties driven by the association between the chain ends and by the strong temperature-sensitivity of the main chain.[13]

Recently, Koizumi et al.[14] carried out a small-angle neutron scattering (SANS) study of solutions of a tel-PNIPAM ($M_n = 22{,}200$ g mol^{-1}) using a newly developed SANS spectrometer with focusing-geometry.[15,16] This instrument achieves a minimum value of measurable wave number in the range of a few 10^{-3} nm^{-1}, which corresponds to ultra-small-angle neutron scattering (USANS), covering a length-scale of almost 1 μm in real space. Here, we use this SANS study to develop a theoretical model of tel-PNIPAM aqueous solutions as they are heated across their cloud points and across the coil-to-globule transition temperature of the PNIPAM chain. We consider the various self-assembled structures of tel-PNIPAMs over a wide concentration region (1 to 50 g L^{-1}) from isolated flower micelles to networks with micellar junctions.

This article first presents a brief summary of the SANS results. Then, these results are interpreted by the theoretical model.[17] By using this model, we quantitatively study the structures of self-assembly on the temperature-concentration plane. Finally, we present a detailed description of the heat-induced progressive transformation of flower micelles into mesoglobules.

Experimental Part

The tel-PNIPAM sample (C_{18}-PNIPAM-C_{18}-22K) was synthesized by reversible addition-fragmentation chain transfer (RAFT) polymerization of NIPAM, as described in reference 9. It consists of a PNIPAM chain terminated at each end with an *n*-octadecyl group. The number-average molecular weight, $M_n = 22{,}200$ g mol^{-1}, and the polydispersity index, $M_w/M_n = 1.16$, were determined using gel permeation chromatography (GPC).[9] The polymerization degree N of PNIPAM was $N = 191$.

SANS and USANS measurements were carried out with a focusing and polarized neutron ultra-small-angle neutron scattering spectrometer (SANS-J-II) at the JRR3 research reactor (20 MW, Japan atomic energy agency (JAEA), Tokai, Japan).[15,16]

Polymer solutions in D_2O (1, 10, and 50 g L^{-1}) were kept at 5 °C for two weeks prior to the measurements to ensure solution homogeneity. The samples were heated from 10 to 40 °C as follows: the solution was brought to a given temperature in small increments (1 to 5 °C), and it was kept at this temperature for 30 min prior to the measurement. SANS data accumulation for each set temperature took approximately 3–4 hours. The sample was then brought to a higher temperature and subjected to the same treatment.

Summary of the Experimental Results

In this section, we present an overview of the temperature and concentration dependence of the SANS profiles.[14] The overall SANS data obtained for solutions of 1, 10, and 50 g L^{-1} are shown in Figure 1. Focusing first on the data of polymer concentration of 10 g L^{-1}, we note that, at low temperature, far below the coil-to-globule transition temperature, the PNIPAM chains are swollen by hydration, while the octadecyl groups aggregate to form the core of the micelles driven by the hydrophobic effect. The main contribution to the SANS intensity originates from such flower micelles at 10 °C. The scattering profile stays almost unchanged from 10 °C to 20 °C. Above 20 °C, the scattering

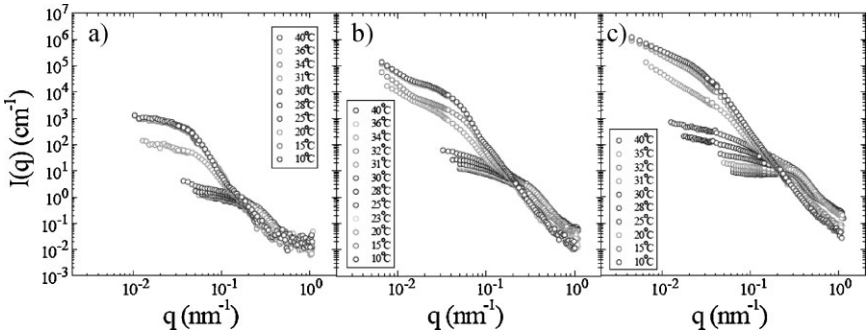

Figure 1.
Neutron scattering profiles at (a) 1, (b) 10, and (c) 50 g L^{-1}. Temperature changes from 10 °C to 40 °C.

intensity in the low q-region ($q < 0.2\,\mathrm{nm}^{-1}$) increases with temperature, indicating association of the micelles. According to previous experiments,[10] the cloud point of this solution lies around 25 °C. Yet, there is no significant change in the scattering profile at this temperature.

At 31 °C, however, the scattering profile drastically changes. There appears a hump at $q \approx 0.05\,\mathrm{nm}^{-1}$, which indicates that large aggregates of the order of 100 nm in size are formed. These aggregates are considered to be ''mesoglobules''.[18–20] Moreover, there is excess scattering exhibiting a power-law in the low q-region ($q < 0.02\,\mathrm{nm}^{-1}$), implying the formation of larger objects via the association of the mesoglobules.

In the case of the solution of the lowest concentration, 1 g L^{-1}, the scattering profile at 10 °C is almost the same as that of 10 g L^{-1} (see Figure 7 for details). The growth of the scattering profile in the low q-region between 20 and 30 °C is less pronounced than that at 10 g L^{-1}. Moreover, there is no excess scattering in the data above 31 °C at 1 g L^{-1}. These findings suggest that the association of micelles or mesoglobules is suppressed in solutions of such low concentration.

The overall temperature dependence of the scattering profile recorded for a solution of 50 g L^{-1} is similar to that of 10 g L^{-1} as shown in Figure 1, except for the appearance of a peak in solutions well below the cloud point due to the correlation between flower micelles.

Theoretical Modelling

In this section, we explain the interpretation of the experimental SANS data by using theoretical models, which are schematically summarized in Figure 2. The mathematical expression of the scattering function of the models is not presented here, due to space limitations. Details of the theoretical models are described in reference 17.

In what follows, we mainly focus on the data at a polymer concentration of 10 g L^{-1}. Since the form of the SANS profile changes with temperature due to the formation of higher order structures, we first consider the lowest temperature, 10 °C, and then move to higher temperatures.

We begin with the data for a polymer concentration of 10 g L^{-1} at 10 °C (Figure 3(d)). At this temperature, the main contribution to the scattering profile originates from individual flower micelles, the formation of which was demonstrated in a previous study.[10] In the low q-region, the scattering profile in Figure 3(d) is, however, somewhat different from the simple summation of individual flower micelles in that it gradually increases with decreasing wave number. We tried to use the conventional core-shell model shown schematically in Figure 3(a), which has been often used for star polymers and polymeric micelles.[5,21] The result of this model, shown in Figure 3 (green line), is almost constant in the region of $q < R_s^{-1}$,

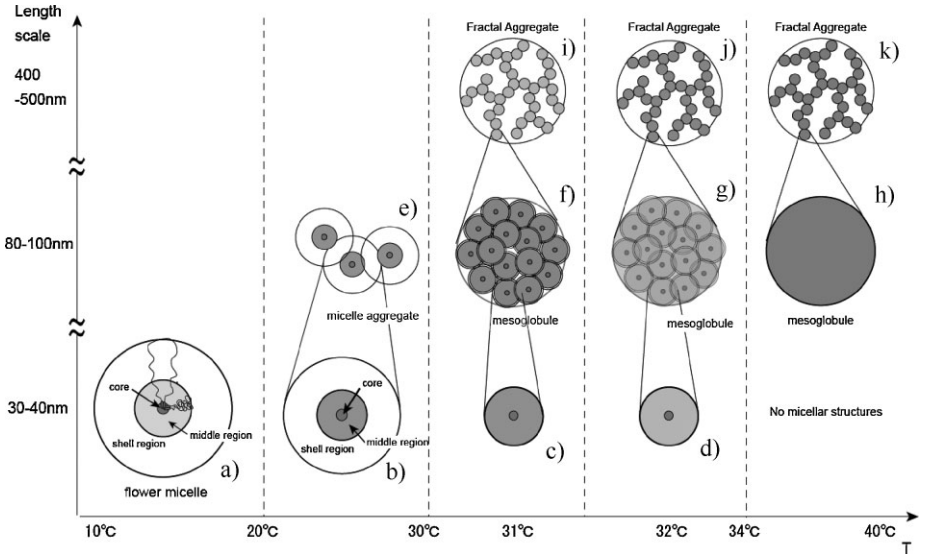

Figure 2.
Theoretical models for hierarchically associated structures of tel-PNIPAM for a solution of 10 g L^{-1}.

and rapidly decreases with q at $q \approx R_s^{-1}$, where R_s is the radius of the micelle (in Figure 3(d), $R_s \approx 15\,\text{nm}$). Although we can adjust R_s to get a better fit in the narrow range around $q \approx 0.3\,\text{nm}^{-1}$, the whole behavior of the scattering data cannot be described by such a simple model.

To improve the fit of the model to the experimental data, we introduce a middle layer in the model. We consider that the PNIPAM chains may partially collapse near the core due to dehydration induced in part by the hydrophobic effect of the end group and in part by the high monomer density close to the core. As a result, there is a region around the core where the density of the PNIPAM chains is much higher than that in the shell region. We call it the middle region. The density profile of the telechelic PNIPAM micelles is hence described by a three layered core-shell model, consisting of the core, middle, and shell regions, as shown in Figure 3(b) and (c).

In order to choose model parameters consistent with the molecular structure, we

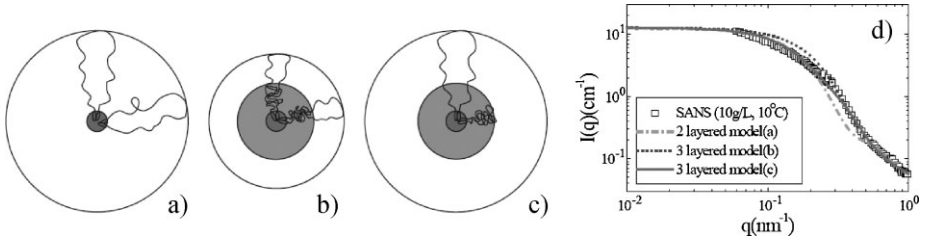

Figure 3.
Core-shell models for flower micelles at a polymer concentration of 10 g L^{-1} and at a temperature of 10 °C. The conformation of the PNIPAM chains in each micelle is schematically drawn. The red circle represents the core consisting of the octadecyl units. (a) Two-layered core-shell model. (b) Three-layered core-shell model with all the PNIPAM chains collapsed near the core. (c) Three-layered core-shell model in which collapsed and swollen PNIPAM chains coexist. (d) Experimental SANS data and plots of the scattering functions according to the three models (a)-(c).

consider the conformation of the PNIPAM chains in the 3-layer core-shell morphology. The simplest model for the conformation of the PNIPAM chains is shown in Figure 3(b), where all the PNIPAM chains of a micelle collapse near the core. However, by careful fitting, we noticed that the shell region of this model was too thin to fit the experimental data as shown in Figure 3(d). To improve this defect, we assume that the collapsed and swollen PNIPAM chains coexist in a micelle as shown in Figure 3(c). This assumption led to a shell radius large enough to reproduce the scattering profile as shown in Figure 3(d). Applying this model to the data in Figure 3(d), we find the aggregation number f of flower micelles in terms of the number of polymer chains to be 12.

As the temperature is increased above 20 °C, the scattering profile in the low q-region is gradually enhanced, compared to the high q-region as shown in Figure 1(b). This change in profile is indicative of association of the flower micelles. We propose the simple model shown in Figure 2(e) to describe the micellar aggregates consisting of flower micelles. We do not explain this model in detail in the present paper, but we find that this model leads to a good fit by comparison with the experimental data shown in Figure 1(b).[17]

In Figure 4, the parameters obtained by the fitting below 30 °C are presented. The fraction $N^{(m)}_{NIPAM}/Nf$ of NIPAM monomer units in the middle layer increases with temperature due to the dehydration of the chains. Simultaneously, the volume fraction of the polymer chains in the middle layer also increases because water molecules are squeezed out of the middle region. As a result, the size R_m of the middle region stays almost constant in the temperature range from 10 to 30 °C. In contrast, the radius of the shell region R_s rapidly decreases with temperature (Figure 4(b)).

As discussed above, the scattering profile drastically changes for solutions heated above 31 °C. The characteristic feature of the high temperature profile is the presence of a hump at $q \approx 0.05\,nm^{-1}$ ascribed to the formation of mesoglobules. It is important to note that the contribution from individual micelles is also observed at $q = 0.2 \sim 0.5\,nm^{-1}$, so that each mesoglobule must consist of many micelles as shown in Figure 5. The scattering from the micelles becomes less prominent for solutions at 32 °C, and completely disappears above 34 °C. This indicates that, with increasing temperature, the micelles dissociate and merge within each mesoglobule.

We construct a model by assuming that a mesoglobule forms a sphere of radius R_{mg}, consisting of N_{mg} micelles (Figure 2(f)). To take the dissociation of micelles into consideration, we also assume that a number g of polymer chains are dissolved and dispersed in a mesoglobule, while the rest of the polymer chains ($f = f_0$-g) remain

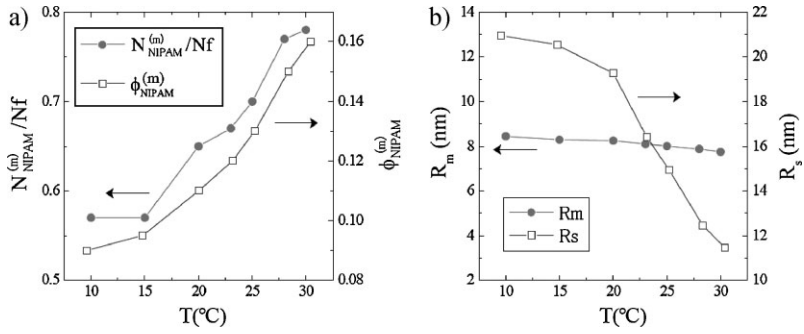

Figure 4.
(a) Temperature dependences of the number $N^{(m)}_{NIPAM}$ of polymer chains collapsed in the middle region and of the volume fraction $\phi^{(m)}_{NIPAM}$ of polymers in the middle region. (b) Temperature dependences of the radii R_m and R_s between T = 10∼30 °C.

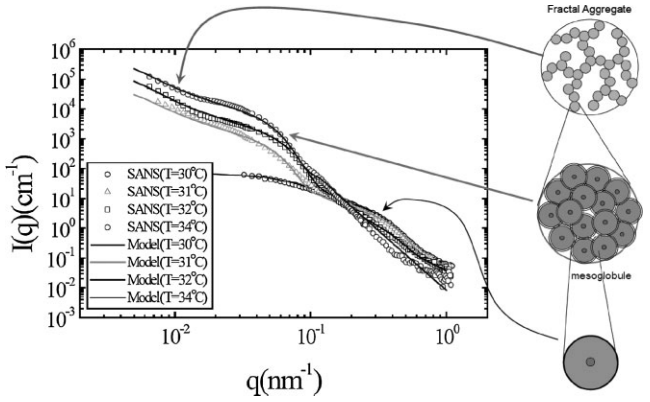

Figure 5.
Comparison between the SANS data (30∼34 °C) and results by the model shown in Figure 2.

in micellar form as schematically shown in Figure 2(f)–(h). We also take into account the contribution from the association of the mesoglobules to explain the power-law behavior q^{-a} ($a \approx 2$) of the intensity at $q < 0.01\ \mathrm{nm}^{-1}$ in the double logarithmic plot as shown in Figure 5. We assume that a fractal aggregate with a fractal dimension $D_f = 2$ consists of N_{fr} mesoglobules (Figure 2(i)–(k)).

In Figure 5, we present a comparison of the theoretical model with the experimental data. The scattering profile is well described by the model with $f/f_0 = 0.67$ at 31 °C. The radius of a mesoglobule was calculated by model fitting[17] to be about $R_{mg} \approx 45\ \mathrm{nm}$, and this value was responsible for the hump appearing at $q \approx 0.05\ \mathrm{nm}^{-1}$ in the scattering profile.

For solutions at 32 °C, we obtain $f/f_0 = 0.42$. This means that 58 percent of the polymer chains in a micelle are dissolved in a mesoglobule. In the case of solutions at 32 °C, we assume that flower micelles completely dissociate in the mesoglobule, i.e., $f = 0$.

In Figure 6, we plot three parameters obtained by the fitting: the mesoglobule-aggregation number N_{agg} (in terms of the number of polymer chains per mesoglobule), the volume fraction $\phi^{(mg)}$ of polymers in the mesoglobules, and the mesoglobule radius R_{mg}. The aggregation number N_{agg} increases with temperature from 31 to 34 °C. Simultaneously, the volume fraction also increases as water molecules are expelled from the mesoglobules. As a result, the size of the mesoglobule remains

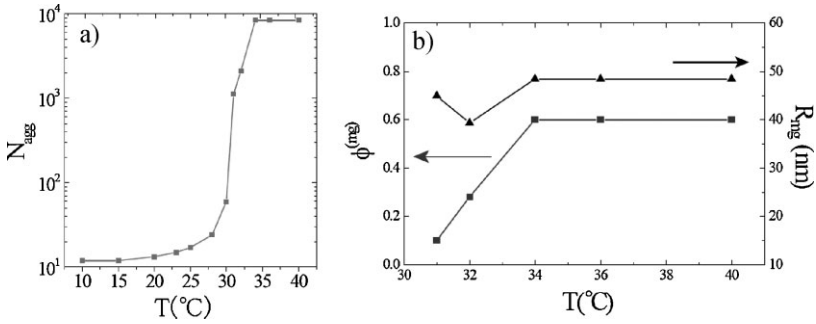

Figure 6.
(a) Temperature dependence of the aggregation number N_{agg} of polymers consisting of a micellar aggregate ($T \leq 30$ °C) and a mesoglobule ($T > 30$ °C). (b) Temperature dependence of the polymer volume fraction $\phi^{(mg)}$ in the mesoglobule and the radius R_{mg} of the mesoglobule.

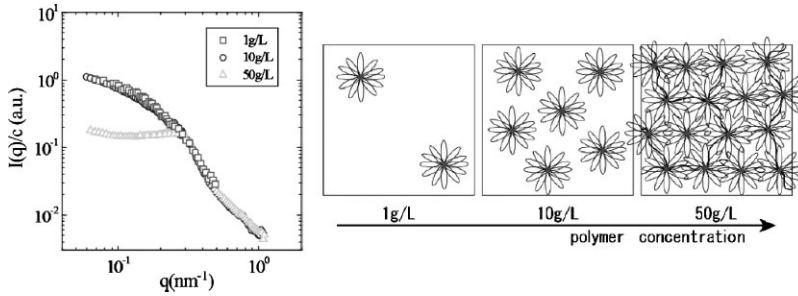

Figure 7.
Concentration dependence of the scattering profiles normalized by the concentration at 10 °C and of the configuration of the micelles.

nearly constant in this temperature region.

Since the scattering profiles do not change above 34 °C, the parameters deduced from them are also independent of temperature. As the coil-to-globule transition proceeds, water molecules bound to the PNIPAM chains are released and squeezed out to the bulk. Then the polymer volume fraction in the mesoglobule becomes large, leading to very slow dynamics of concentration fluctuations within the mesoglobules such that the structure becomes almost frozen at 34 °C.

We next discuss the concentration dependence of the associated structure. Scattering profiles recorded in the low temperature region, normalized by the polymer concentration of 1, 10 and 50 g L^{-1} at 10 °C, are presented in Figure 7. The plot for the solution of 1 g L^{-1} is almost identical to that for 10 g L^{-1}, implying that the structure of micelles is independent of concentration between 1 g L^{-1} and 10 g L^{-1}. Hence the number of micelles in solutions of concentration of 1 g L^{-1} is the 1/10 of that in solutions of concentration of 10 g L^{-1}.

For the solution of 50 g L^{-1}, the scattering profile presents a peak at $q_{max} \approx 0.25\,nm^{-1}$, due to the correlation between different flower micelles. From the peak position, the distance between micelles is roughly estimated as $l \approx 2\pi/q_{max} \approx 24\,nm^{-1}$, leading to $f \approx cN_A\, l^3/M_n \approx 19$ for the aggregation number f of micelles. Although this value is somewhat higher than the value obtained in the more dilute regions (1 and 10 g L^{-1}), the result ($f \approx 19$) does not differ appreciably. Moreover, since the scattering profile in the high q-region ($q > 0.25\,nm^{-1}$) for solutions of 50 g L^{-1} agrees well with that for solutions of 10 g L^{-1}, the internal structure of micelles is believed to be almost the same from 10 g L^{-1} to 50 g L^{-1}.

The scattering data in the high temperature range normalized by the concentration are presented in Figure 8, and compared with the theoretical model with $N_{fr} = 1$ with other parameters being the same as those for 10 g L^{-1}. The scattering profiles at 1 g L^{-1} show no excess scattering at low $q < 0.03\,nm^{-1}$. This behavior is also observed in the scattering profiles above 31 °C at 1 g L^{-1} as shown in Figure 1(a). Since the excess scattering at low q is

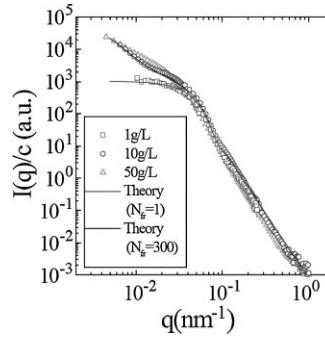

Figure 8.
Polymer concentration dependence of the scattering profiles at 40 °C normalized by the concentration. The fractal models with $N_{fr} = 1$ and 300 are also shown (solid lines).

interpreted as the contribution of associated mesoglobules, the SANS data indicate that association of mesoglobules does not take place at 1 g L^{-1}. The good agreement between the experimental data and theory implies that the structure of the mesoglobules is the same as that at 10 g L^{-1}.

For 50 g L^{-1}, the scattering profile at $q > 0.05\,nm^{-1}$ is almost the same as that of the two lower concentrations, indicating that the structure of the mesoglobules is nearly identical. The intensity in the low $q < 0.05\,nm^{-1}$ region for 50 g L^{-1} is slightly greater than that for 10 g L^{-1}, implying that the association of the mesoglobules at 50 g L^{-1} is more pronounced compared to 10 g L^{-1}. Thus, we find that, at high temperatures, the structure of the mesoglobules formed is independent of concentration, whereas the association of the mesoglobules depends on concentration.

Conclusion

We have constructed a theoretical model to account for the temperature and polymer concentration dependence of the SANS profiles recorded for solutions of telechelic PNIPAM. This model enabled us to propose a consistent description of the self-assembled structures of telechelic PNIPAM in D_2O over wide temperature and polymer concentration ranges. A pictorial representation of the temperature-concentration dependence of the solutions is summarized in the form of a phase diagram in Figure 9. Telechelic PNIPAMs associate in the form of flower micelles in dilute solutions at low temperatures. A molecular model of a flower micelle consisting of 12 tel-PNIPAM chains constructed with the aid of molecular modeling software is presented in Figure 10. Each of the tel-PNIPAM polymer molecules consists of 190 NIPAM units and two octadecyl units, one at each end. On heating, collapse of the PNIPAM chains by dehydration starts near the core of the flower micelles, and this eventually leads to the association of the micelles. Flower micelles were described by a three-layered core-shell structure. The scattering intensities recorded above 31 °C unambiguously indicate the presence of isolated mesoglobules, already reported in the case of dilute PNIPAM homopolymer solutions.[18–20] The mesoglobules remain stable far above the cloud point, but the hydrophobic cores of the individual micelles may not be preserved within each mesoglobule.

In solutions of high polymer concentration, we have observed a peak in the

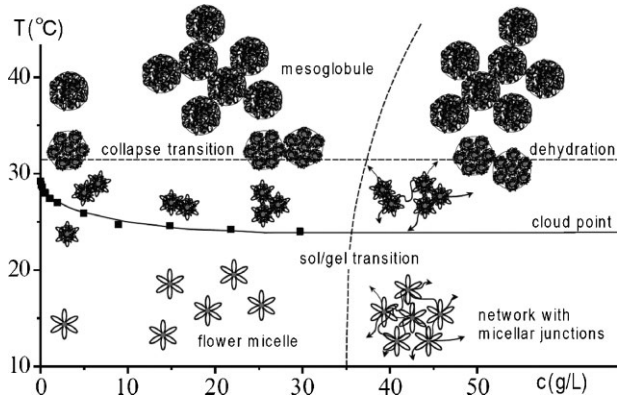

Figure 9.
Temperature-polymer concentration phase diagram of telechelic PNIPAMs in water, indicating the collapse transition temperature (dashed line), the cloud-point line (solid line), the sol/gel transition line (dashed line), together with associated structures such as flower micelles, mesoglobules, flowers connected by bridging chains, and aggregates of mesoglobules.

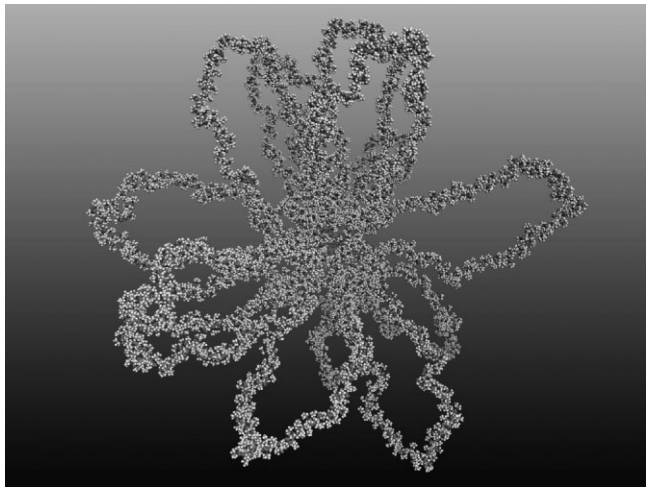

Figure 10.
Molecular model of a flower micelle consisting of 12 tel-PNIPAM molecules, each of which comprising 190 NIPAM units and two octadecyl groups, one at each end.

scattering profile due to the correlation between flower micelles at low temperature, which can be interpreted as micellar packing. The effects of such network formation cannot be assessed by static SANS experiments only. We expect that the rheological properties of micellar networks connected by bridging chains are much different from those of dense uncrosslinked micellar solutions.

[1] "*Hydrophilic Polymers: Performance with Environmental Acceptability*t", J. E. Glass, Ed., American Chemical Society, Washington, DC Vol. *248*, 1996.
[2] "*Associative Polymers in Aqueous Solution*", J. E. Glass, Ed., American Chemical Society, Washington, DC Vol. *765*, 2000.
[3] M. A. Winnik, A. Yekta, *Curr. Opin. Colloid Interface Sci.* **1997**, *2*, 424 and references therein.
[4] Y. Séréro, R. Aznar, G. Porte, J.-F. Berret, D. Calvet, A. Collet, M. Viguier, *Phys. Rev. Let.* **1998**, *81*, 5584; Y. Séréro, V. Jacobsen, J.-F. Berret, R. May, *Macromolecules* 2000, *33*, 1841.
[5] E. Beaudoin, O. Borisov, A. Lapp, L. Billon, R. C. Hiorns, J. Francois, *Macromolecules* **2002**, *35*, 7436.
[6] T. Annable, R. Buscall, R. Ettelaie, D. Whittlestone, *J. Rheology* **1993**, *37*, 695.
[7] J.-F. Berret, Y. Séréro, B. Winkelman, D. Calvet, A. Collet, M. Viguier, *J. Rheology* **2001**, *45*, 477; J.-F. Berret, Y. Séréro, *Phys. Rev. Lett.* 2001, *87*, 048303.
[8] P. Kujawa, H. Watanabe, F. Tanaka, F. M. Winnik, *Eur. Phys. J. E* **2005**, *17*, 129.
[9] P. Kujawa, F. Segui, S. Shaban, C. Diab, Y. Okada, F. Tanaka, F. M. Winnik, *Macromolecules* **2006**, *39*, 341.
[10] P. Kujawa, F. Tanaka, F. M. Winnik, *Macromolecules* **2006**, *39*, 3048.
[11] Y. Okada, F. Tanaka, P. Kujawa, F. M. Winnik, *J. Chem. Phys.* **2006**, *125*, 244902.
[12] H. G. Schild, *Prog. Polym. Sci.* **1992**, *17*, 163.
[13] Y. Okada, F. Tanaka, *Macromolecules* **2005**, *38*, 4465.
[14] R. Motokawa, S. Koizumi, T. Koga, F. Tanaka, F. M. Winnik (in preparation).
[15] S. Koizumi, H. Iwase, J. Suzuki, T. Oku, R. Motokawa, H. Sasao, H. Tanaka, D. Yamaguchi, H. M. Shimizu, T. Hashimoto, *J. Appl. Cryst.* **2007**, *40*, s474.
[16] S. Koizumi, H. Iwase, J. Suzuki, T. Oku, R. Motokawa, H. Sasao, H. Tanaka, D. Yamaguchi, H. M. Shimizu, T. Hashimoto, *Physica B* **2006**, *385*, 1000.
[17] T. Koga, F. Tanaka, R. Motokawa, S. Koizumi, F. M. Winnik, *Macromolecules* **2008**, *41*, 9413.
[18] C. Balu, M. Delsanti, P. Guenoun, F. Monti, M. Cloitre, *Langmuir* **2007**, *23*, 2404.
[19] G. Zhang, C. Wu, *Adv. Polym. Sci.* **2006**, 195. 101, and references therein.
[20] V. O. Aseyev, H. Tenhu, F. M. Winnik, *Adv. Polym. Sci.* **2006**, 196. 1, and references therein.
[21] M. Daoud, J. P. Cotton, *J. Physique* **1982**, *43*, 531.

